Biochemistry and Biophysics Reports 26 (2021) 100995

Contents lists available at ScienceDirect

Biochemistry and Biophysics Reports

journal homepage: www.elsevier.com/locate/bbrep

Green synthesis and characterization of zinc oxide nanoparticles using Cayratia pedata leaf extract

Ashwini Jayachandran *, Aswathy T.R., Achuthsankar S. Nair

Department of Computational Biology & Bioinformatics, University of Kerala, Kariyavattom Campus, Thiruvananthapuram, Kerala, 695581, India

ARTICLE INFO

Keywords:
Green synthesis
Zinc oxide nanoparticles
Cayratia pedata

ABSTRACT

The synthesis of Zinc oxide nanoparticles using a plant-mediated approach is presented in this paper. The nanoparticles were successfully synthesized using the Nitrate derivative of Zinc and plant extract of the indigenous medicinal plant *Cayratia pedata.* 0.1 mM of Zn $(NO_3)_2.6H_2O$ was made to react with the plant extract at different concentrations, and the reaction temperature was maintained at 55 °C, 65 °C, and 75 °C. The yellow coloured paste obtained was wholly dried, collected, and packed for further analysis. In the UV visible spectrometer (UV–Vis) absorption peak was observed at 320 nm, which is specific for Zinc oxide nanoparticles. The characterization carried out using Field Emission Scanning Electron Microscope (FESEM) reveals the presence of Zinc oxide nanoparticles in its agglomerated form. From the X-ray diffraction (XRD) pattern, the average size of the nanoparticles was estimated to be 52.24 nm. Energy Dispersive Spectrum (EDX) results show the composition of Zinc and Oxygen, giving strong energy signals of 78.32% and 12.78% for Zinc and Oxygen, respectively. Fourier Transform - Infra-Red (FT-IR) spectroscopic analysis shows absorption peak of Zn–O bonding between 400 and 600 cm^{-1}. The various characterization methods carried out confirm the formation of nano Zinc oxide. The synthesized nanoparticles were used in the immobilization of the enzyme Glucose oxidase. Relative activity of 60% was obtained when Glucose oxidase was immobilized with the green synthesized ZnO nanoparticles. A comparative study of the green synthesized with native ZnO was also carried out. This green method of synthesis was found to be cost-effective and eco-friendly.

1. Introduction

There has been a tremendous increase in nanotechnology in the past decade due to its application in medicine, chemistry, and biotechnology [1–3]. Progress in this field has opened new horizons in nanoscience, particularly in drug delivery, gene delivery, nanomedicine, biosensing, etc. [4,5]. One of the unique properties that make nano-sized particles so interesting is their high surface-to-volume ratio [6]. This feature of nanoparticles enables them to be more reactive than the bulk material as atoms on the surface tend to be more active than those at the center [7,8]. These nanoparticles are synthesized using physical, chemical, or biological methods. Various physical and chemical methods like hydrothermal, sol-gel synthesis, laser ablation, lithography, etc., require special equipment and skilled labor. Moreover, they have toxic effects that are hazardous to health. The nanoparticles obtained via the green synthesis method are found to be cost-effective, non-toxic, and biodegradable in nature [9–12]. This ecofriendly synthesis method reduces the use of hazardous substances as the process utilizes natural materials like leaves, roots, and flower extracts and microorganisms like bacteria, fungi, algae, etc. [13–15].

Recent studies show the significance of green synthesis of metal oxide nanoparticles where oxides of metals like zinc, gold, copper, silver, nickel, etc., are gaining importance [16–18]. Our point of interest is to synthesize nanoparticles that can be utilized in the realization of optical biosensors, which favors materials with good optical properties like optical absorption, optical emission, photoluminescence, chemiluminescence, etc. [19,20]. Of the various metal oxides, ZnO nanoparticles exhibit high electron mobility, large exciton binding energy, wide bandgap, and high optical transmittance [21,22]. These optical properties of zinc oxide are utilized in sensor fabrication [23–25].

The present work focuses on the green synthesis method of producing ZnO nanoparticles from the plant *Cayratia pedata,* commonly known as 'Birdfoot Grapevine'', which belongs to the family *Vitaceae* [26]. *Cayratia pedata* is an indigenous endangered medicinal plant seen in the southern part of India. It is a woody climber with a cylindrical stem and

* Corresponding author.
E-mail addresses: ashwinijayachandrans@gmail.com (A. Jayachandran), aswathyravikumartr@gmail.com (A. T.R.), achuthsankar@keralauniversity.ac.in (A.S. Nair).

https://doi.org/10.1016/j.bbrep.2021.100995
Received 29 August 2019; Received in revised form 24 February 2021; Accepted 25 March 2021

Abbreviations

ZnO	Zinc oxide
$Zn(NO_3)_2 .6H_2O$	Zinc nitrate hexahydrate
EDX	Energy Dispersive Spectrometry
FESEM	Field Emission Scanning Electron Microscopy
UV–Vis	UV–Visible Spectroscopy
FT-IR	Fourier Transform - Infra Red Spectroscopy
ICDD	International Centre for Diffraction Data®
XRD	X-ray Diffraction Spectrometry
FWHM	Full width half maximum

grows mostly in tropical forests. Traditionally, the leaf of the plant is used in the treatment of ulcers, inflammation, and scabies [27]. The plant extract is rich in alkaloids, tannins, phenolic compounds, flavonoids, and terpenoids [28]. The crude extracts of the plant have varying degree of antimicrobial [29], anti-ulcer [30], anti-inflammatory [31], anti-arthritic [32], anti-diarrheal [33], anti-oxidant [34] and anti-nociceptive [35] properties. This is the first attempt to synthesis ZnO nanoparticles from *Cayratia pedata.* However, *Cayratia pedata* was used as a reducing agent in the past to synthesize silver nanoparticles [36].

The synthesized nanoparticles can be used for various applications like sensors, lasers, drug discovery, etc., and the synergistic effects may be measured depending on the application. In such applications where the anticancer [37], antibacterial [38], antimicrobial [39], anti-tyrosinase [40], and antibiofilm [41] activities of nanoparticles are utilized, shape and size play an important role. For example, when compared to rod-shaped ZnO NP, the spherically shaped NP can release Zn^{2+} ions with much ease, and small-sized particles are more permeable to bacteria membranes [42–44]. Furthermore, ZnO nanoparticles are found to be a better catalyst that can be recycled with lesser degradation in its activity [45]. There are a lot many applicational areas where the properties of nanoparticles can be utilized. However, these nanoparticles reported in our work were synthesized specifically to immobilize the enzyme glucose oxidase to develop it as a biosensor further. Immobilization using the green synthesis method has been reported in the past [46]. However, this is the first work where green synthesized ZnO nanoparticles were used for immobilizing the enzyme glucose oxidase, which is specific to glucose.

1.1. Mechanism of plant-mediated approach

The green synthesis mechanism for the synthesis of ZnO nanoparticles is depicted in Fig. 1. The phytochemicals present in the plant extract can act as reducing agents for converting the metal precursors to metal nanoparticles. Phytochemicals are antioxidants and toxic-free chemicals; hence they can act as both reducing and stabilizing agents [47]. The essential phytochemicals such as Terpenoids, Flavonoids, Phenolic compounds, Aldehydes, and Alkaloids have contributed to the reducing process. These phytochemical reducing agents vary at different concentrations in different types of plant extracts. So the leaf extract composition has a significant effect on nanoparticle synthesis. The factors such as pH, temperature, contact time, metal salt concentration, and phytochemical profile of plant extract affect the nanoparticle synthesis, nanoparticle stabilization, and the quantity of nanoparticle produced [48]. Makarov et al. proposed that the metal ions will be encapsulated as an organic covering in three steps for their stabilization after reduction by plant extracts. 1. Activation phase: involves metal ion reduction and nucleation of reduced metal ions, 2. Growth phase: involved in nanoparticle stability, 3. The termination phase: consists of the shape of nanoparticles formed [49]. Metals such as copper, silver, gold titanium, zinc, iron, and nickel result in the formation of their metal oxides by the activity of phytochemicals. By the action of phytochemicals, metal ions achieve the growth and stabilization phase. The formation of oxygen finally results in the linking of metal ions, and a defined shape is formed.

The processes involved in the plant-based extraction mechanism of nanoparticle synthesis are preparation of the plant extract, mixing of the metallic solution in the plant extract, and the formation of biocompatible nanoparticles. Then the characterization of the nanoparticles was done by FTIR, SEM, TEM, XRD, etc., the details of which are explained in the following session.

2. Materials and methods

2.1. Materials

Fresh *Cayratia pedata* var. *glabra* plant (Voucher no: KUBH10096) was collected from Thiruvananthapuram (8.5241 N, 76.9366 E) and identified by a taxonomist at the Department of Botany, University of Kerala. The chemical Zinc nitrate hexahydrate (98% purity) used for the analysis was purchased from Merck®.

2.2. Preparation of extract

The leaves of the plant are washed thoroughly with distilled water to remove dust and other particles. The washed plant part is then dried at room temperature. 50 gm of leaves were weighed and taken for analysis. They were sliced into small pieces and are crushed using a mortar and pestle by adding a sufficient amount of water. The extract is prepared at two different concentrations - Sample A (25 gm in 50 ml) and Sample B (25 gm in 100 ml) to study the effect of concentration variation in sample preparation. The extract was then pretreated by boiling it for 15 min, which softens the cell membrane, followed by filtering using Whatman No. 1 filter paper. In order to remove the debris, it is then centrifuged at 2400 rpm for 5 min, and the supernatant is taken for further experimentation.

2.3. Green synthesis of nanoparticles

Modified procedures of previous work on green synthesis to produce ZnO nanoparticles have been taken for the study, which is reported in Table 1. The critical aspects of all these procedures reported here were

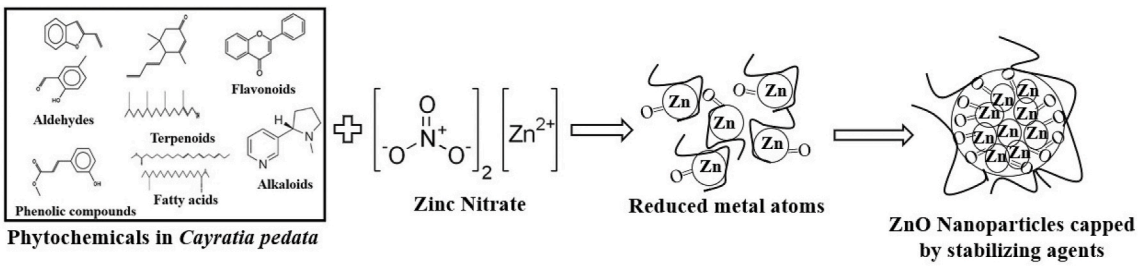

Fig. 1. Green synthesis mechanism for producing ZnO nanoparticles.

Table 1
Modified procedures of various studies taken as reference for our study.

Sl No.	Plant/fungi/ bacteria (Concentration),	Filtering process/pre heating	Working temperature and condition	References
1	*Brassica oleracea* L. *var. Italic* (8g in 80 ml)	At 70 °C for 20 min	Heated at 70 °C for 20 min + centrifuged at 6000 rpm for 20 min + dried at 80 °C for 6 h + calcinated at 450 °C	[50]
2	*Deverra tortuosa* (crude extract of 25 ml)	At 60–80 °C	Heated at 60 °C overnight + paste collected and heated at 400 °C for 2 h	[51]
3	*Euphorbia petiolata* (50g in 500 ml)	At 80 °C for 30 min	Heated at 80 °C for 2 h + centrifuged at 6000 rpm + annealing at 400 °C for 2 h	[52]
4	*Punica granatum* L. (40g)	At 40 °C at pH 3 and filtered with Whatman filter paper (0.22 m)	Heated at 80 °C + centrifuged at 1000 rpm for 10 min annealing at 400 °C and 500 °C	[53]
5	*Mussaenda frondosa* (1:10)	At 100 °C for 4 h	Stirring at 450–500 rpm + mix heated at 400 °C for 10–30 min in magnetic stirrer	[54]
6	*Eucalyptus globulus Labill* (20g in 100 ml)	At 60 °C in oven and cooled to room temperature	Centrifuged at 5000 rpm for 1 h + calcined at 400 °C for 2 h	[55]

considered for the present work. When compared to other synthesis procedures where Zinc nitrate was regarded as the precursor, this study tried to minimize the complexity in processes carried out, amount of chemicals used, and the time taken for the analysis without deteriorating the quality of the synthesized nanoparticle. 5 ml of 10 mM Zn $(NO_3)_2.6H_2O$ was poured into the homogeneous leaf extracts prepared, and the mixture is stirred at 65 °C for 20 min. Both sample A and sample B.

having turned light yellow were then collected and allowed to heat overnight at the same temperature until a thick yellow paste was obtained. This paste was then dried completely and calcined at 400 °C for 2 h before collecting and packing separately for further characterization. Calcination removes the impurities present in the sample, and you get a purified form of the NP, and the process is temperature-dependent [56]. The sample had undergone various evaluation and measurements like UV visible spectrometer, SEM, XRD, EDX, and FT-IR to finally confirm it as ZnO nanoparticles. This procedure was repeated for 55 °C and 75 °C, temperatures above and below the working temperature. While experimenting with 55 °C, the reaction between Zinc Nitrate and plant extract was not happening, resulting in nano ZnO formation. Moreover, when used 75 °C as the working temperature, it formed ashes because the temperature was too high. However, at 65 °C, a yellow colour change was observed without any side effects. Moreover, while doing characterization, the sample was confirmed to be ZnO nanoparticles. Hence the temperature plays an important role in the formation of nanoparticles. Fig. 2 shows the various stages of ZnO nanoparticle synthesis using the plant extract of *Cayratia pedata*.

2.4. Characterization of zinc oxide nanoparticles

2.4.1. UV–visible spectroscopy

The optical property of synthesized ZnO nanoparticles was observed from the absorption spectra of nanoparticles synthesized at various temperatures and concentrations. This is characterized using an Ultraviolet–Visible Spectrometer (Cary Series, Agilent Technology) with a wavelength in the range of 200 nm–800 nm. UV light for LEDs can also be used for spectroscopy purposes. They are of three types. UV A (400 nm–315nm), UV B (315 nm–280 nm) and UV C (280 nm −100 nm. Latter is more environmentally friendly, but the former is better in cost-effectiveness and can be used for generic purposes. So, we chose UV–Visible spectroscopy for our analysis as UV-LEDs are application-specific.

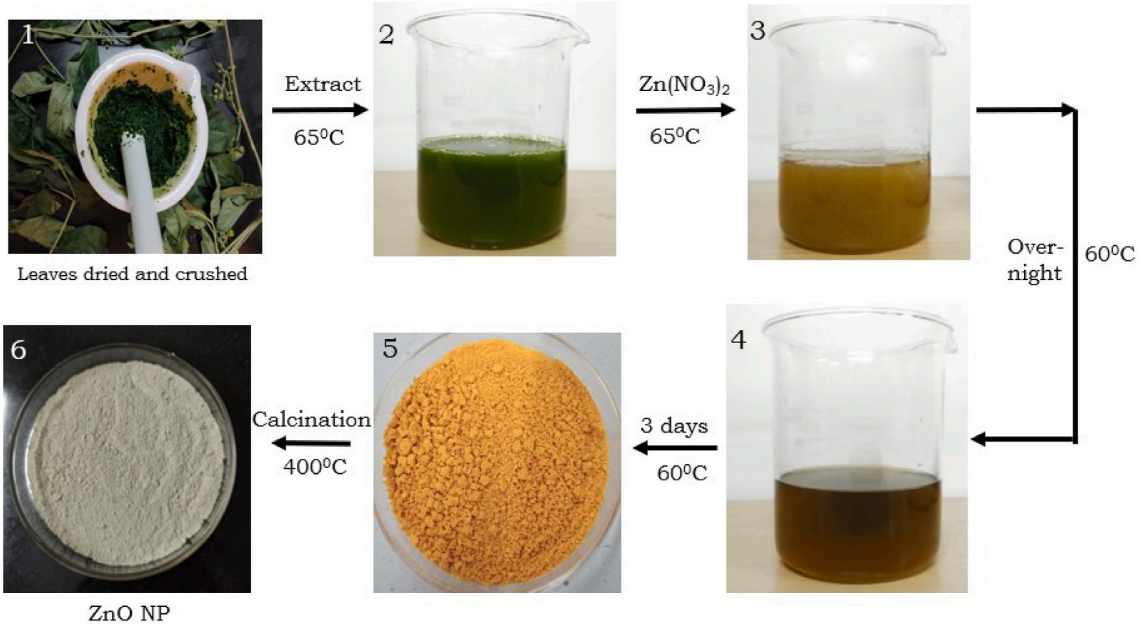

Fig. 2. Stages of green synthesis of Zinc oxide nanoparticles from Zinc nitrate precursor using the plant extract of *Cayratia pedata* as reducing agent. (For interpretation of the references to colour in this figure legend, the reader is referred to the Web version of this article.)

2.4.2. Scanning electron microscopy

Nova NanoSEM 450 analyzer with acceleration voltage 10 KV was used to take the images of biosynthesized zinc oxide nanoparticles. For taking the FESEM images, the synthesized particles were mixed with acetone and allowed to dry on a glass slide in order to get a thin layer for the analysis.

X-Ray Diffractogram:

Analysis of the crystalline material is carried out using X-Ray Diffractometer - Bruker AXS D8 Advance, with Cu k-alpha radiation of wavelength 1.5402 A^0.

2.4.3. Energy dispersive spectrometry

Energy dispersive spectrometry was used for getting the elemental details of the nanomaterial and its composition.

2.4.4. Fourier transform infrared spectroscopy

The infrared absorption spectrum produced by this characterization technique reveals the chemical bonds in the synthesized nanoparticles. For this, FT-IR Spectrophotometer-ThermoFisher-Scientific Nicolet iS50 was used for the analysis.

2.4.5. Enzyme immobilization

After confirming the synthesized particles as nano ZnO using various characterization, the nanoparticles produced were used in the immobilization of the enzyme. Glucose oxidase was immobilized on synthesized ZnO nanoparticles by a simple adsorption method. For the adsorption process, 1 mg of GOx was added to 0.1 M sodium acetate buffer of pH-5. To the above solution, 0.5 g of ZnO nanoparticles were added and incubated overnight at 30 °C with constant stirring. The experiment was carried out for other values of pH – 3, 7, and 9. After immobilization, the Glucose oxidase activity was determined using the assay kit to know how much enzymes are active after the process. The assay was based on hydrogen peroxide production by the immobilized Glucose oxidase's enzymatic reaction on the substrate glucose. The formed hydrogen peroxide reaction with fluorescent peroxidase substrate is colorimetrically measured at 570 nm.

3. Results and discussion

3.1. UV–visible spectroscopy

The presence of secondary metabolites in plants reduces zinc ions in the solution to zinc oxide. The plant extract not only acts as reducing agents but as stabilizing agents as well. This was confirmed by taking the UV–visible spectrum analysis in the range of 280 nm–800 nm. The spectrum showed a peak at 320 nm, which is specific for ZnO nanoparticles. For ZnO nanoparticles, the absorbance peak is reported between 310 nm and 360nm of wavelength [57]. Sample A shows more absorption owing to a higher concentration of plant extract. The graph in Fig. 3 that denotes a smaller absorption peak corresponds to sample B. In sample B itself, two absorption peaks can be seen. One with a slightly higher absorption peak indicates sample B when it was initially taken for the analysis. The lowermost graph of sample B shows that the nanoparticles settle down at the bottom as time increases, and hence absorption decreases. As sample A showed more absorbance due to higher concentration, that sample was considered for further characterization. The bandgap energy was calculated using $Eg = 1240/\lambda$ eV and found to be 3.8 eV which is comparable to the previously reported values of energy bandgap for ZnO nanoparticles [58,59].

3.2. FESEM analysis

FESEM images were taken in different magnifications to examine the shape and size of the nanoparticles synthesized, as shown in Fig. 4. The surface morphology confirms the formation of nanoparticles in their agglomerated form. Various literature reports the effect of surface morphology and its relationship in the synergistic activity of ZnO [60]. The particles were found to be mostly horizontal in shape, which was further confirmed using XRD.

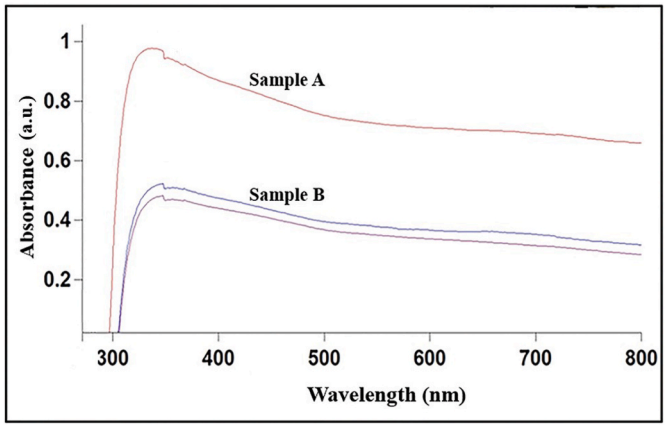

Fig. 3. UV–Vis spectra for Zinc oxide nanoparticles at two different concentrations.

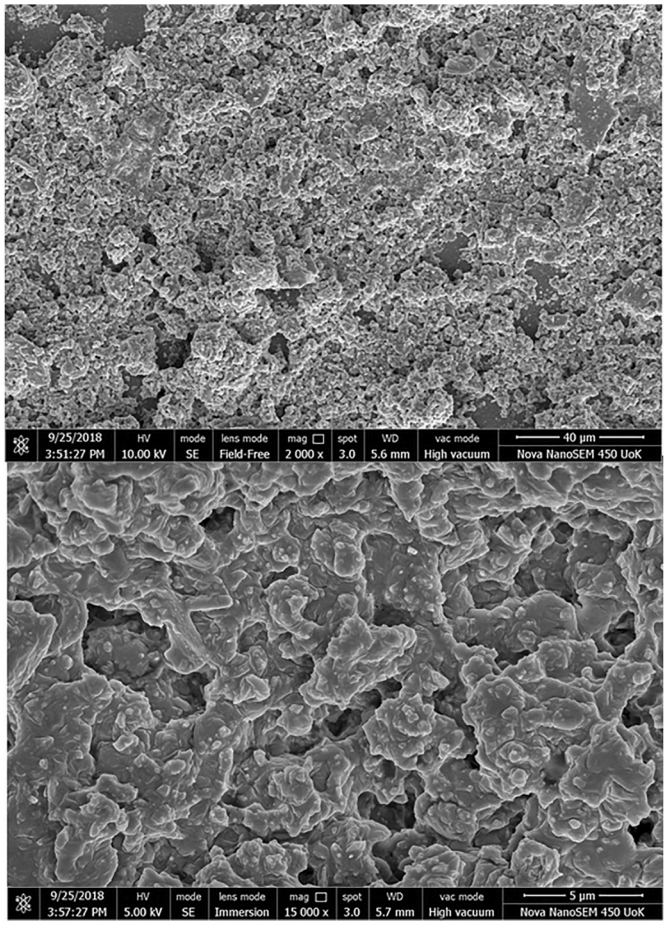

Fig. 4. FESEM image of ZnO nanoparticles at various magnification.

3.3. XRD analysis

XRD gives the crystalline nature of ZnO nanoparticles. The diffractogram shows the intensity of the diffracted rays as a function of diffraction angles. The spectra show the details of the crystal planes. Corresponding to the lattice planes (100), (002), (101), (102), (110),

(103), (112), and (201), as shown in Fig. 5, the x-ray diffraction peaks were obtained at various angles as detailed in Table 2. The size of the nanoparticles was measured using the Debye-Scherrer equation

$$D = \frac{k\lambda}{\beta\cos\theta}\text{Å}$$

where D is the average crystalline particle size, λ is the wavelength of x-ray (1.5406 Å), k is the shape factor or Scherer's constant (0.9), θ is Bragg's diffraction angle, and β is the XRD peak full width at half maximum.

Using Scherrer's formula, the average crystalline size of the nanoparticles formed was estimated and found to be 52.24 nm. The peaks were matched with the ICDD card number 01-079-0207. The shape of the nanoparticles was found to be hexagonal in nature with lattice parameters a (=b) equal to 3.2568 A^0 and c equal to 5.2125 A^0, which matches with the values previously reported [61,62].

3.4. EDX analysis

EDX revealed a high signal for Zinc and Oxygen, which confirms the presence of Zinc in the oxide form. The composition of each element contained in the analyte is obtained from the EDX, which gives strong peaks of 78.32% for Zinc and 12.78% for Oxygen, whose weight% peaks are comparable to that reported earlier for the synthesis of ZnO nanoparticles [63]. Two strong peaks were identified for Zinc at 1eV and 8.6 eV, and for Oxygen, the signal was evident at 0.5 eV [64,65].

These values are specific for Zinc and Oxygen, which confirms the elemental composition of the compound synthesized. Apart from Zinc and Oxygen, there were traces of other compounds like Sodium, which is shown in Fig. 6.

3.5. FT-IR analysis

FT-IR gives the composition and formation of functional groups of the synthesized ZnO nanoparticles. It also suggests that the formation of ZnO nanoparticles is due to the interaction of the phenolic compounds, alkynes, terpenoids, and flavonoids. Fig. 7 represents FT-IR spectra of the synthesized ZnO nanoparticles in the range 400–4000 cm^{-1}. The functional groups were responsible for reducing zinc ions to ZnO, which was observed as bands. Each of the bands corresponds to various stretching modes.

Table 2
Results of XRD analysis at various diffraction angles.

Sl. No.	2Θ	FWHM (β)	Miller indices	Particle size (D)
1	31.57	0.00230	(100)	60.30
2	34.24	0.00230	(002)	60.30
3	36.07	0.00234	(101)	59.27
4	47.36	0.00244	(102)	56.84
5	56.42	0.00279	(110)	49.75
6	62.69	0.00300	(103)	46.23
7	67.77	0.00326	(112)	42.55
8	68.91	0.00325	(201)	42.71

The broad band observed at 3275 cm^{-1} corresponds to O–H stretching of phenolic compounds [66]. The alkene group's presence was attributed to 1624 cm^{-1} [67], and the band at 1313 cm^{-1} corresponds to C–N stretching bonds of the amines [68]. The C–O stretching of esters and carboxylic functional groups and the bands between 1000 and 1300 corresponds, and the multiple sharp bands at 491 cm^{-1} and 435 cm^{-1} are attributed to the presence of Zn–O stretching bands [69, 70].

3.6. Immobilization of enzyme

GOx activity at all values of pH showed activity greater than 50%, as shown in Fig. 8. The least activity was seen at pH 3. However, the highest activity of about 60% was observed at pH5, where Sodium Acetate was used as the buffer with green synthesized ZnO nanoparticles. Thereafter a slight decrease in activity was exhibited from pH 5 to pH 9. The relative activity at various pH values was compared with the enzyme activity when adsorbed using native ZnO, which gave the highest relative activity of 68%. This value was comparable with the enzyme activity reported earlier for the immobilization of a cysteine functionalized enzyme immobilization using ZnO nanoparticles [71]. Unlike the green synthesized method, the least activity was observed at pH 7 for native ZnO. But for both ZnO nanoparticles, the highest activity was observed at a pH of 5. This could be extended to optimize various other parameters like temperature, concentration, etc.

4. Conclusion

The study reports a simple, cost-efficient, and greener method for synthesizing Zinc oxide from the leaves extract of the plant *Cayratia*

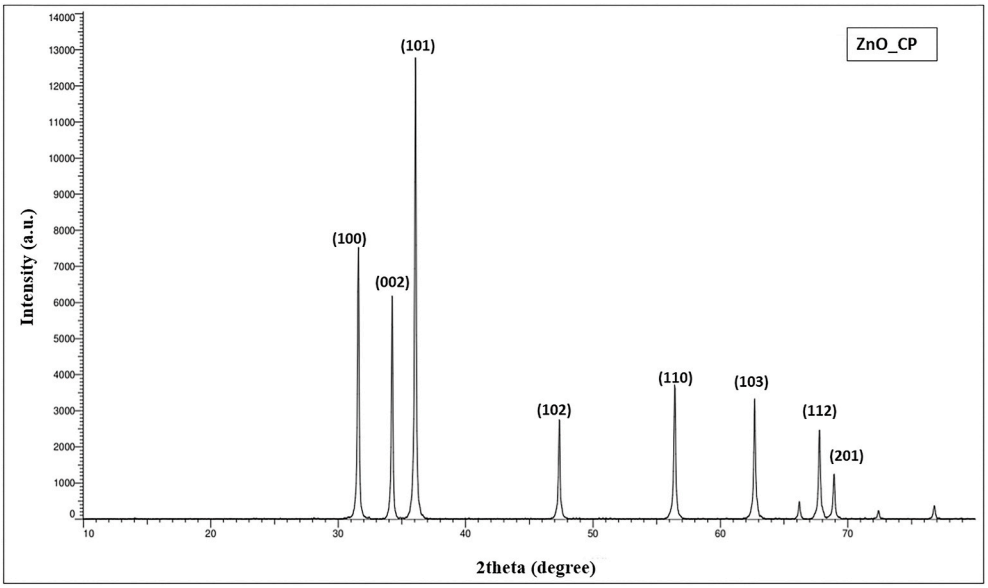

Fig. 5. X-ray diffraction spectrum of synthesized Zinc oxide nanoparticles.

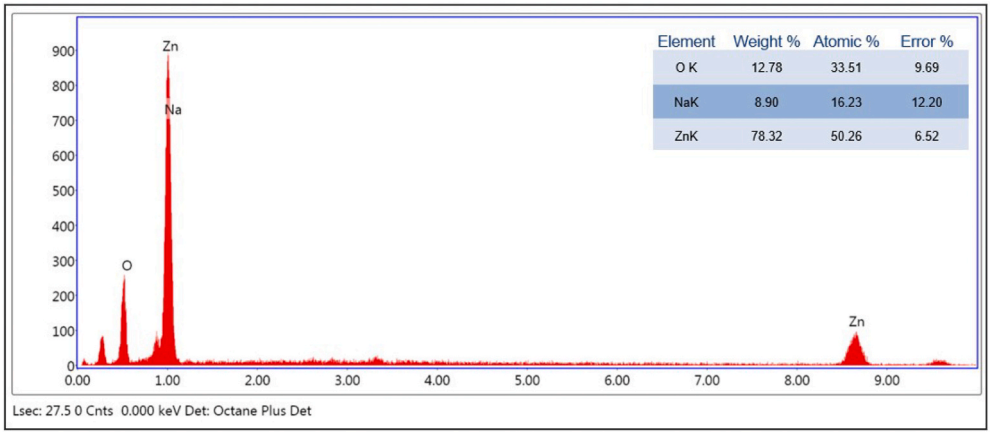

Fig. 6. EDX spectrum of synthesized Zinc oxide nanoparticles.

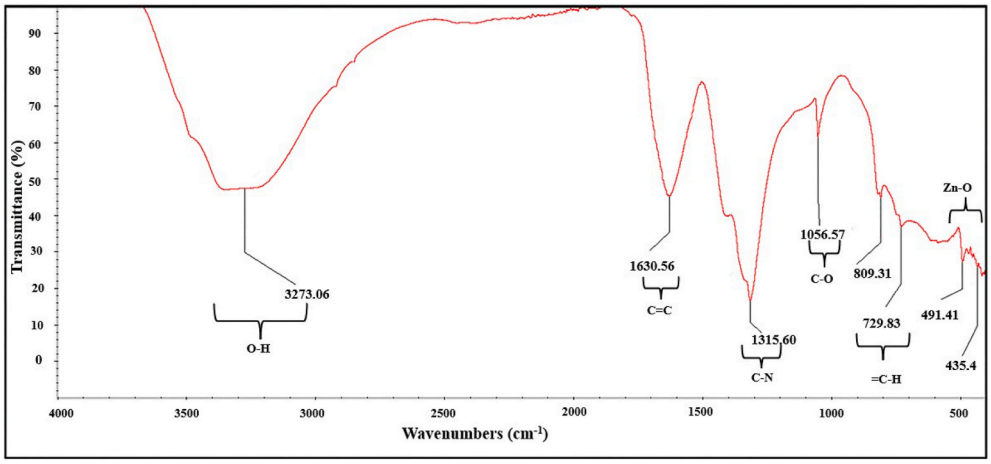

Fig. 7. FTIR spectrum of synthesized Zinc oxide nanoparticles.

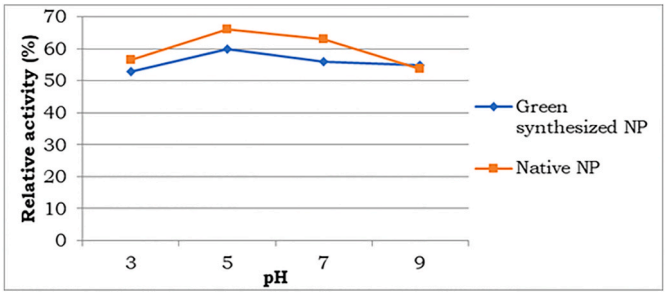

Fig. 8. Enzyme activity profile of glucose oxidase at different pH, using green synthesized nanoparticles and native nanoparticles. (For interpretation of the references to colour in this figure legend, the reader is referred to the Web version of this article.)

Pedata. Unlike the conventional techniques used to produce the nanoparticles, the green synthesis method was found to be ecofriendly and can be achieved by less usage of chemicals. Nano Zinc oxide of varying sizes was obtained through wet chemical synthesis, and the average size was found to be 52.24 nm. SEM analysis confirms the ZnO's size and structure, whose purity and composition were determined by EDX studies. The stretching and bonding were examined through FT-IR spectroscopy, and the shape and average size of the nanoparticles formed were investigated using XRD analysis. The synthesized ZnO nanoparticles gave a relative activity of 60% when used for enzyme immobilization, which is 88.2% of the activity compared to native ZnO immobilization.

Authors contribution

AJ carried out research, conceptualization, and experimentation on the green synthesis of nanoparticles. Studies on the plant *Cayratia pedata* and its formal analysis was carried out by ATR and ASN was the supervising guide who contributed to writing, reviewing, analyzing the data and acquisition of fund. All authors read and approved the final manuscript.

Declaration of competing interest

All authors declare that they do not have any conflict of interest. They also declare that this manuscript has not been published elsewhere and is not under consideration by another journal.

Acknowledgements

The authors would like to acknowledge University Grants Commission, New Delhi, Department of Biotechnology-Bioinformatics Infrastructure facility (DBT-BIF), Ministry of Human resource development-Ayurinformatics Computer-Aided Drug Design (MHRD-AiCADD), State Inter-University Centre for Excellence in Bioinformatics (SIUCEB), Department of Computational Biology and Bioinformatics for their support and Central Laboratory for instrumentation and facilitation

(CLIF), the University of Kerala for extending necessary facilities in sample analysis for the completion of the work.

References

[1] M. Singh, S. Singh, S. Prasad, I.S. Gambhir, Nanotechnology in medicine and antibacterial effect of silver nanoparticles, Dig. J. Nanomater. Bios. 3 (2008) 115–122.

[2] G.M. Whitesides, Nanoscience, nanotechnology, and chemistry, Small 1 (2005) 172–179, https://doi.org/10.1002/smll.200400130.

[3] B. Pelaz, S. Jaber, D.J. De Aberasturi, V. Wulf, T. Aida, J.M. de la Fuente, N. A. Kotov, The state of nanoparticle-based nanoscience and biotechnology: progress, promises, and challenges, ACS Nano 6 (2012) 8468–8483, https://doi.org/10.1021/nn303929a.

[4] C. Jianrong, M. Yuqing, H. Nongyue, W. Xiaohua, L. Sijiao, Nanotechnology and biosensors, Biotechnol. Adv. 22 (2004) 505–518, https://doi.org/10.1016/j.biotechadv.2004.03.004.

[5] X. Zhang, Q. Guo, D. Cui, Recent advances in nanotechnology applied to biosensors, Sensors 9 (2009) 1033–1053, https://doi.org/10.3390/s90201033.

[6] B.D. Yao, Y.F. Chan, N. Wang, Formation of ZnO nanostructures by a simple way of thermal evaporation, Appl. Phys. Lett. 81 (2002) 757–759, https://doi.org/10.1063/1.1495878.

[7] Y. Yin, R.M. Rioux, C.K. Erdonmez, S. Hughes, G.A. Somorjai, A.P. Alivisatos, Formation of hollow nanocrystals through the nanoscale Kirkendall effect, Science 304 (2004) 711–714, https://doi.org/10.1126/science.1096566.

[8] J.V. Barth, G. Costantini, K. Kern, Engineering atomic and molecular nanostructures at surfaces, in: Nanoscience and Technology: A Collection of Reviews from Nature Journals, 2010, pp. 67–75, https://doi.org/10.1142/9789814287005_0008.

[9] J. Virkutyte, R.S. Varma, Green synthesis of metal nanoparticles: biodegradable polymers and enzymes in stabilization and surface functionalization, Chem. Sci. 2 (2011) 837–846, https://doi.org/10.1039/C0SC00338G.

[10] M.N. Nadagouda, R.S. Varma, Green synthesis of silver and palladium nanoparticles at room temperature using coffee and tea extract, Green Chem. 10 (2008) 859–862, https://doi.org/10.1039/B804703K.

[11] M. Darroudi, Z. Sabouri, R.K. Oskuee, A.K. Zak, H. Kargar, M.H.N.A. Hamid, Green chemistry approach for the synthesis of ZnO nanopowders and their cytotoxic effects, Ceram. Int. 40 (2014) 4827–4831, https://doi.org/10.1016/j.ceramint.2013.09.032.

[12] S. Iravani, Green synthesis of metal nanoparticles using plants, Green Chem. 13 (2011) 2638–2650, https://doi.org/10.1039/C1GC15386B.

[13] M. Behravan, A.H. Panahi, A. Naghizadeh, M. Ziaee, R. Mahdavi, A. Mirzapour, Facile green synthesis of silver nanoparticles using Berberis vulgaris leaf and root aqueous extract and its antibacterial activity, Int. J. Biol. Macromol. 124 (2019) 148–154, https://doi.org/10.1016/j.ijbiomac.2018.11.101.

[14] P. Rajiv, S. Rajeshwari, R. Venkatesh, Bio-Fabrication of zinc oxide nanoparticles using leaf extract of Parthenium hysterophorus L. and its size-dependent antifungal activity against plant fungal pathogens, Spectrochim. Acta Mol. Biomol. Spectrosc. 112 (2013) 384–387, https://doi.org/10.1016/j.saa.2013.04.072.

[15] G.R. Navale, M. Thripuranthaka, D.J. Late, S.S. Shinde, Antimicrobial activity of ZnO nanoparticles against pathogenic bacteria and fungi, JSM Nanotechnol Nanomed 3 (2015) 1033.

[16] J.S. Moodley, S.B.N. Krishna, K. Pillay, P. Govender, Green synthesis of silver nanoparticles from Moringa oleifera leaf extracts and its antimicrobial potential, Adv. Nat. Sci. Nanosci. Nanotechnol. 9 (2018), 015011.

[17] I.M. Chung, A. Abdul Rahuman, S. Marimuthu, A.K. Vishnu Kirthi, P. Anbarasan, Padmini G. Rajakumar, Green synthesis of copper nanoparticles using Eclipta prostrata leaves extract and their antioxidant and cytotoxic activities, Exp Ther Med. 14 (2017) 18–24, https://doi.org/10.3892/etm.2017.4466.

[18] J. Suresh, G. Pradheesh, V. Alexramani, M. Sundrarajan, S.I. Hong, Green synthesis and characterization of zinc oxide nanoparticle using insulin plant (Costus pictus D. Don) and investigation of its antimicrobial as well as anticancer activities, Adv. Nat. Sci. Nanosci. Nanotechnol. 9 (2018), 015008, https://doi.org/10.1088/2043-6254/aaa6f1.

[19] C.L. Baird, D.G. Myszka, Current and emerging commercial optical biosensors, J. Mol. Recogn. 14 (2001) 261–268, https://doi.org/10.1002/jmr.544.

[20] J. Shi, Y. Zhu, X. Zhang, W.R. Baeyens, A.M. Garcıa-Campana, Recent developments in nanomaterial optical sensors, Trends Anal. Chem. 23 (2004) 351–360, https://doi.org/10.1016/S0165-9936(04)00519-9.

[21] G. Sangeetha, S. Rajeshwari, R. Venckatesh, Green synthesis of zinc oxide nanoparticles by aloe barbadensis miller leaf extract: structure and optical properties, Mater. Res. Bull. 46 (2011) 2560–2566, https://doi.org/10.1016/j.materresbull.2011.07.046.

[22] A. Kołodziejczak-Radzimska, T. Jesionowski, Zinc oxide—from synthesis to application: a review, Materials 7 (2014) 2833–2881, https://doi.org/10.3390/ma7042833.

[23] T.V. Kolekar, S.S. Bandgar, S.S. Shirguppikar, V.S. Ganachari, Synthesis and characterization of ZnO nanoparticles for efficient gas sensors, Arch. Appl. Sci. Res. 5 (2013) 20–28.

[24] Z.Q. Zheng, J.D. Yao, B. Wang, G.W. Yang, Light-controlling, flexible and transparent ethanol gas sensor based on ZnO nanoparticles for wearable devices, Sci. Rep. 5 (2015) 1107, https://doi.org/10.1038/srep11070.

[25] S. Yedurkar, C. Maurya, P. Mahanwar, Biosynthesis of zinc oxide nanoparticles using ixora coccinea leaf extract—a green approach, Open J. Synth. Theor. Appl. 5 (2016) 1, https://doi.org/10.4236/ojsta.2016.51001.

[26] C.P. Khare, Indian Medicinal Plants- an Illustrated Dictionary, 1st Indian Reprint Springer Pvt. Ltd., New Delhi, India, 2007.

[27] K.S. Manilal, Vaan Rheede's Hortus Malabaricus with Annotation and Modern Botanical Nomenclature, Bangalore, 2003.

[28] A.L. Stanley, V.A. Ramani, A. Ramachandran, Phytochemical screening and GC-MS studies on the ethanolic extract of Cayratia pedata, Int. J. Pharm. Phytopharmacol. Res. 1 (2012) 112–116.

[29] K. Nayak, J. Lazar, Antimicrobial efficacy of leaf extract of Cayratia pedata Lam, Vitaceae. Int. J. Chemtech res. 6 (2014) 5721–5725.

[30] P. Karthik, P. Amudha, J. Srikanth, Study on phytochemical profile and antiulcerogenic effect of Cayratia pedata Lam in albino wistar rats, J. Pharmacol. (Paris) 2 (2010) 1017–1029.

[31] V. Rajendran, V. Rathinambal, V. Gopal, A preliminary study on anti-inflammatory activity of Cayratia pedata leaves on Wister albino rats, Der. Pharmacia. Lettre. 3 (2011) 433–437.

[32] K. Selvarani, G.V.S. Bai, Anti-arthritic activity of Cayratia pedata leaf extract in Freund's adjuvant induced arthritic rats, Int. J. Res. Pharm. Sci. 4 (2014) 55–59.

[33] P. Karthik, R.N. Kumar, P. Amudha, Anti-diarrheal activity of the chloroform extract of Cayratia pedata Lam in albino wistar rats, J. Pharmacol. (Paris) 2 (2011) 69–75.

[34] C. Rice-Evans, N. Miller, G. Paganga, Antioxidant properties of phenolic compounds, Trends Plant Sci. 2 (1997) 152–159, https://doi.org/10.1016/S1360-1385(97)01018-2.

[35] V. Rajendran, S. Indumathy, V. Gopal, Anti-nociceptive activity of Cayratia pedata in experimental animal models, J. Pharm. Res. 4 (2011) 852–853.

[36] V. Subramani, J.J. Jeyakumar, M. Kamaraj, B. Ramachandran, Plant extracts derived silver nanoparticles, Int. J. Pharmaceut. Sci. Rev. Res. 3 (2014) 16–19.

[37] M.D. Jayappa, C.K. Ramaiah, M.A.P. Kumar, D. Suresh, A. Prabhu, R.P. Devasya, S. Sheikh, Green synthesis of zinc oxide nanoparticles from the leaf, stem and in vitro grown callus of Mussaenda frondosa L.: characterization and their applications, Appl. Nanosci. 10 (2020) 3057–3074.

[38] M. Naseer, U. Aslam, B. Khalid, B. Chen, Green route to synthesize Zinc Oxide Nanoparticles using leaf extracts of Cassia fistula and Melia azadarach and their antibacterial potential, Sci. Rep. 10 (2020) 1–10.

[39] N. Supraja, T.N.V.K.V. Prasad, A.D. Gandhi, D. Anbumani, P. Kavitha, R. Babujanarthanam, Synthesis, characterization and evaluation of antimicrobial efficacy and brine shrimp lethality assay of Alstonia scholaris stem bark extract mediated ZnONPs, Biochemistry and biophysics reports 14 (2018) 69–77.

[40] M. Darroudi, S. Ranjbar, M. Esfandiar, M. Khoshneviszadeh, M. Hamzehloueian, M. Khoshneviszadeh, Y. Sarrafi, Synthesis of novel triazole incorporated thiazolone motifs having promising antityrosinase activity through green nanocatalyst CuI-Fe3O4@ SiO2 (TMS-EDTA), Appl. Organomet. Chem. 34 (2020), e5962.

[41] P.P. Mahamuni, P.M. Patil, M.J. Dhanavade, M.V. Badiger, P.G. Shadija, A. C. Lokhande, R.A. Bohara, Synthesis and characterization of zinc oxide nanoparticles by using polyol chemistry for their antimicrobial and antibiofilm activity, Biochemistry and biophysics reports 17 (2019) 71–80.

[42] S. Alamdari, M. Sasani Ghamsari, C. Lee, W. Han, H.H. Park, M.J. Tafreshi, H. Afarideh, M.H.M. Ara, Preparation and characterization of zinc oxide nanoparticles using leaf extract of Sambucus ebulus, Appl. Sci. 10 (2020) 3620, https://doi.org/10.3390/app10103620.

[43] Y.H. Leung, C.M.N. Chan, A.M.C. Ng, H.T. Chan, M.W.L. Chiang, Antibacterial activity of ZnO nanoparticles with a modified surface under ambient illumination, Nanotechnology 23 (2012) 475703, https://doi.org/10.1088/0957-4484/23/47/475703.

[44] M. Arakha, M. Saleem, B.C. Mallick, S. Jha, The effects of interfacial potential on antimicrobial propensity of ZnO nanoparticles, Sci. Rep. 5 (2015) 9578, https://doi.org/10.1038/srep09578.

[45] K.V.V. Satyanarayana, P.A. Ramaiah, Y.L.N. Murty, M.R. Chandra, S.V.N. Pammi, Recyclable ZnO nano particles: economical and green catalyst for the synthesis of A3 coupling of propargylamines under solvent free conditions, Catal. Commun. 25 (2012) 50–53, https://doi.org/10.1016/j.catcom.2012.03.031.

[46] M. Švecová, O. Volochanskyi, M. Dendisová, D. Palounek, P. Matějka, Immobilization of green-synthesized silver nanoparticles for micro-and nano-spectroscopic applications: what is the role of used short amino-and thio-linkers and immobilization procedure on the SERS spectra? Spectrochim. Acta Mol. Biomol. Spectrosc. 247 (2021) 119142.

[47] J. Singh, T. Dutta, K.H. Kim, M. Rawat, P. Samddar, P. Kumar, 'Green'synthesis of metals and their oxide nanoparticles: applications for environmental remediation, J. Nanobiotechnol. 16 (2018) 1–24, https://doi.org/10.1186/s12951-018-0408-4.

[48] K.S. Mukunthan, S. Balaji, Cashew apple juice (Anacardium occidentale L.) speeds up the synthesis of silver nanoparticles, Int. J. Green Nanotechnol. 4 (2012) 71–79, https://doi.org/10.1080/19430892.2012.676900.

[49] A.J. Love, V.V. Makarov, O.V. Sinitsyna, J. Shaw, I.V. Yaminsky, N.O. Kalinina, M. A. Taliansky, Genetically modified tobacco mosaic virus that can produce gold nanoparticles from a metal salt precursor, Front. Plant Sci. 6 (2015) 984, https://doi.org/10.3389/fpls.2015.00984.

[50] J. Osuntokun, D.C. Onwudiwe, E.E. Ebenso, Green synthesis of ZnO nanoparticles using aqueous Brassica oleracea L. var. italica and the photocatalytic activity, Green Chem. Lett. Rev. 12 (2019) 444–457, https://doi.org/10.1080/17518253.2019.1687761.

[51] M. Aminuzzaman, L.P. Ying, W.S. Goh, A. Watanabe, Green synthesis of zinc oxide nanoparticles using aqueous extract of Garcinia mangostana fruit pericarp and their photocatalytic activity, Bull. Mater. Sci. 41 (2018) 50, https://doi.org/10.1007/s12034-018-1568-4.

[52] C. Mohammadi, S. Mahmud, S.M. Abdullah, Y. Mirzaei, Green synthesis of ZnO nanoparticles using the aqueous extract of Euphorbia petiolata and study of its

stability and antibacterial properties, Moroc. J. Chem. 5 (2017), https://doi.org/10.48317/IMIST.PRSM/morjchem-v5i3.8974, 5-3.
[53] X. Fuku, A. Diallo, M. Maaza, Nanoscaled electrocatalytic optically modulated ZnO nanoparticles through green process of Punica granatum L. and their antibacterial activities, Int. J. Electrochem. (2016), https://doi.org/10.1155/2016/4682967.
[54] M.D. Jayappa, C.K. Ramaiah, M.A.P. Kumar, D. Suresh, A. Prabhu, R.P. Devasya, S. Sheikh, Green synthesis of zinc oxide nanoparticles from the leaf, stem and in vitro grown callus of Mussaenda frondosa L.: characterization and their applications, Appl. Nanosci. (2020) 1–18, https://doi.org/10.1007/s13204-020-01382-2.
[55] A.A. Barzinjy, H.H. Azeez, Green synthesis and characterization of zinc oxide nanoparticles using Eucalyptus globulus Labill. leaf extract and zinc nitrate hexahydrate salt, SN Applied Sciences 2 (2020) 1–14.
[56] R. Nayak, Ali, D.K. Mishra, D. Ray, V.K. Aswal, S.K. Sahoo, B. Nanda, Fabrication of CuO nanoparticle: an efficient catalyst utilized for sensing and degradation of phenol, J. Mater. Res. 9 (2020) 11045–11059, https://doi.org/10.1016/j.jmrt.2020.07.100.
[57] M. Sasani Ghamsari, S. Alamdari, W. Han, H. Park, Impact of nanostructured thin ZnO film in ultraviolet protection, Int. J. Nanomed. 12 (2016) 207–216, https://doi.org/10.2147/IJN.S118637.
[58] S.T. Tan, B.J. Chen, X.W. Sun, W.J. Fan, H.S. Kwok, X.H. Zhang, S.J. Chua, Blueshift of optical band gap in ZnO thin films grown by metal-organic chemical-vapor deposition, J. Appl. Phys. 98 (2005), 013505, https://doi.org/10.1063/1.1940137.
[59] M.K. Debanath, S. Karmakar, Study of blueshift of optical band gap in zinc oxide (ZnO) nanoparticles prepared by low-temperature wet chemical method, Mater. Lett. 111 (2013) 116–119, https://doi.org/10.1016/j.matlet.2013.08.069.
[60] X. Peng, S. Palma, N.S. Fisher, S.S. Wong, Effect of morphology of ZnO nanostructures on their toxicity to marine algae, Aquat. Toxicol. 102 (2011) 186–196, https://doi.org/10.1016/j.aquatox.2011.01.014.
[61] S.T. Fardood, A. Ramazani, S. Moradi, P.A. Asiabi, Green synthesis of zinc oxide nanoparticles using Arabic gum and photocatalytic degradation of direct blue 129 dye under visible light, J. Mater. Sci. Mater. Electron. 28 (2017) 13596–13601, https://doi.org/10.1007/s10854-017-7199-5.
[62] R. Vinayagam, R. Selvaraj, P. Arivalagan, T. Varadavenkatesan, Synthesis, characterization and photocatalytic dye degradation capability of Calliandra haematocephala-mediated zinc oxide nanoflowers, J. Photochem. Photobiol. B Biol. 203 (2020) 111760, https://doi.org/10.1016/j.jphotobiol.2019.111760.
[63] S. Pai, H. Sridevi, T. Varadavenkatesan, R. Vinayagam, R. Selvaraj, Photocatalytic zinc oxide nanoparticles synthesis using Peltophorum pterocarpum leaf extract and their characterization, Optik 185 (2019) 248–255, https://doi.org/10.1016/j.ijleo.2019.03.101.
[64] W.N. Unertl, J.M. Blakely, Growth and properties of oxide films on Zn (0001), Surf. Sci. 69 (1977) 23–52, https://doi.org/10.1016/0039-6028(77)90160-1.
[65] S. Fakhari, M. Jamzad, H. Kabiri Fard, Green synthesis of zinc oxide nanoparticles: a comparison, Green Chem. Lett. Rev. 12 (2019) 19–24, https://doi.org/10.1080/17518253.2018.1547925.
[66] M. Ganesh, S.G. Lee, J. Jayaprakash, M. Mohankumar, H.T. Jang, Hydnocarpus alpina Wt extract mediated green synthesis of ZnO nanoparticle and screening of its anti-microbial, free radical scavenging, and photocatalytic activity, Biocatal Agric Biotechnol 19 (2019) 101129, https://doi.org/10.1016/j.bcab.2019.101129.
[67] D. Hu, W. Si, W. Qin, J. Jiao, X. Li, X. Gu, Y. Hao, Cucurbita pepo leaf extract induced synthesis of zinc oxide nanoparticles, characterization for the treatment of femoral fracture, J. Photochem. Photobiol. B Biol. 195 (2019) 12–16, https://doi.org/10.1016/j.jphotobiol.2019.04.001.
[68] K.D. Sirdeshpande, A. Sridhar, K.M. Cholkar, R. Selvaraj, Structural characterization of mesoporous magnetite nanoparticles synthesized using the leaf extract of Calliandra haematocephala and their photocatalytic degradation of malachite green dye, Appl. Nanosci. 8 (2018) 675–683.
[69] C. Chen, B. Yu, P. Liu, J. Liu, L. Wang, Investigation of nano-sized ZnO particles fabricated by various synthesis routes, J. Ceram. Process. Res. 12 (2011) 420–425.
[70] J. Lu, I. Batjikh, J. Hurh, Y. Han, H. Ali, R. Mathiyalagan, D.C. Yang, Photocatalytic degradation of methylene blue using biosynthesized zinc oxide nanoparticles from bark extract of Kalopanax septemlobus, Optik 182 (2019) 980–985, https://doi.org/10.1016/j.ijleo.2018.12.016.
[71] N. Verma, N. Kumar, L.S.B. Upadhyay, R. Sahu, A. Dutt, Fabrication and characterization of cysteine-functionalized zinc oxide nanoparticles for enzyme immobilization, Anal. Lett. 50 (11) (2017) 1839–1850.